Supplementary information

Ultra-flexible temperature-insensitive strain sensor

Yu Kato, Kenjiro Fukuda, Takao Someya, Tomoyuki Yokota**

Y. Kato, T. Someya, T. Yokota

Department of Electrical Engineering and Information Systems, The University of Tokyo, 7-3-1 Hongo, Bunkyo-ku, Tokyo 113-8656, Japan

E-mail: someya@ee.t.u-tokyo.ac.jp (T.S.); yokota@ntech.t.u-tokyo.ac.jp (T.Y.)

K. Fukuda, T. Someya

Center for Emergent Matter Science, RIKEN, 2-1 Hirosawa, Wako, Saitama 351-0198, Japan

K. Fukuda, T. Someya

Thin-Film Device Laboratory, RIKEN, 2-1 Hirosawa, Wako, Saitama 351-0198, Japan

T. Yokota

Institute of Engineering Innovation, Graduate School of Engineering, The University of Tokyo, 7-3-1 Bunkyo-ku, Tokyo, 113–8656, Japan

Table S1 Comparison of the performance of near-zero-TCR strain sensors that can apply strain to sensor materials through bending substrates. The minimum bending radii in some references were not illustrated or other methods were used to apply strain; therefore, the estimated values from the following formula are shown: $r = d_s/2\varepsilon$, where r is the minimum bending radius, d_s is the substrate thickness, and ε is the maximum applied strain. Remarkably, our sensor was thin and showed good flexibility in comparison. The TCR of 0.11% K^{-1} was sufficient to suppress the temperature effects, as demonstrated in this study.

Ref.	Sensor material	Process (Solution processes are underlined)	Substrate material	Substrate thickness	Maximum applied strain	TCR	Minimum bending radius
1	ITO, Pt	Sputtering	Zirconia	Unknown	0.0256%	−0.0079% K^{-1}	Unknown
2	Au, graphene	Transferring	Polyimide	30 µm	Unknown	Unclear	Unknown
3	ITO, Ag	Sputtering	Al_2O_3	380 µm	Unknown	~0.05% K^{-1} *	750 mm (Experiment)
4	Au	Evaporation	PET	100 µm	<0.75%	Unclear	>6.7 mm (Estimation)
5	RuO_2, glass powder	<u>Printing</u>	Al_2O_3	Unknown	Unknown	~0.01% K^{-1} *	Unknown
6	MWCNT, graphene	<u>Drop casting</u>	Polyimide	Unknown	~0.24%	−0.0218 Ω K^{-1}	Unknown
7	CNT, Ag NPs	<u>Screen printing</u>	PET	100 µm	Unknown	~0.03% K^{-1}	Unknown
8	SWCNT, graphite	<u>Spray coating</u>	PET	250 µm	0.16%	Unclear	78 mm (Estimation)
9	Au NPs, ITO NPs	<u>Spin coating</u>	PDMS/PET	800/50 µm	1.8%	−0.00007989% K^{-1}	24 mm (Estimation)
10	Ag NPs	<u>Spin coating</u>	PET	250 µm	1%	0.0019% K^{-1}	13 mm (Estimation)
11	GNPs, Polysilazane	<u>Direct ink writing</u>	Paper	100 µm	0.5%	0.002% K^{-1}	10 mm (Estimation)
12	PEDOT:PSS	<u>Spin coating</u>	PET/PDMS	50/1000 µm	5%	0.0093% /K^{-1}	1.25 mm (ε=2%, Experiment) 0.5 mm (ε=5%, Estimation)
This study	**P3HT, BCF, Ag NPs**	**<u>Spin coating</u>**	**Polyimide**	**12.5 µm**	**6.1%**	**0.11% K^{-1}**	**0.14 mm (Experiment)**

*Specific numbers are unclear

ITO: indium tin oxide, PET: polyethylene terephthalate, MWCNT: multi-walled carbon nanotube, CNT: carbon nanotube, NP: nanoparticle, SWCNT: single-walled carbon nanotube, PDMS: polydimethylsiloxane, GNPs: graphite nanoplatelets, PEDOT: poly(3,4-ethylenedioxythiophene), PSS: poly(styrenesulfonate), P3HT: poly(3-hexylthiophene-2,5-diyl), BCF: tris(pentafluorophenyl)borane

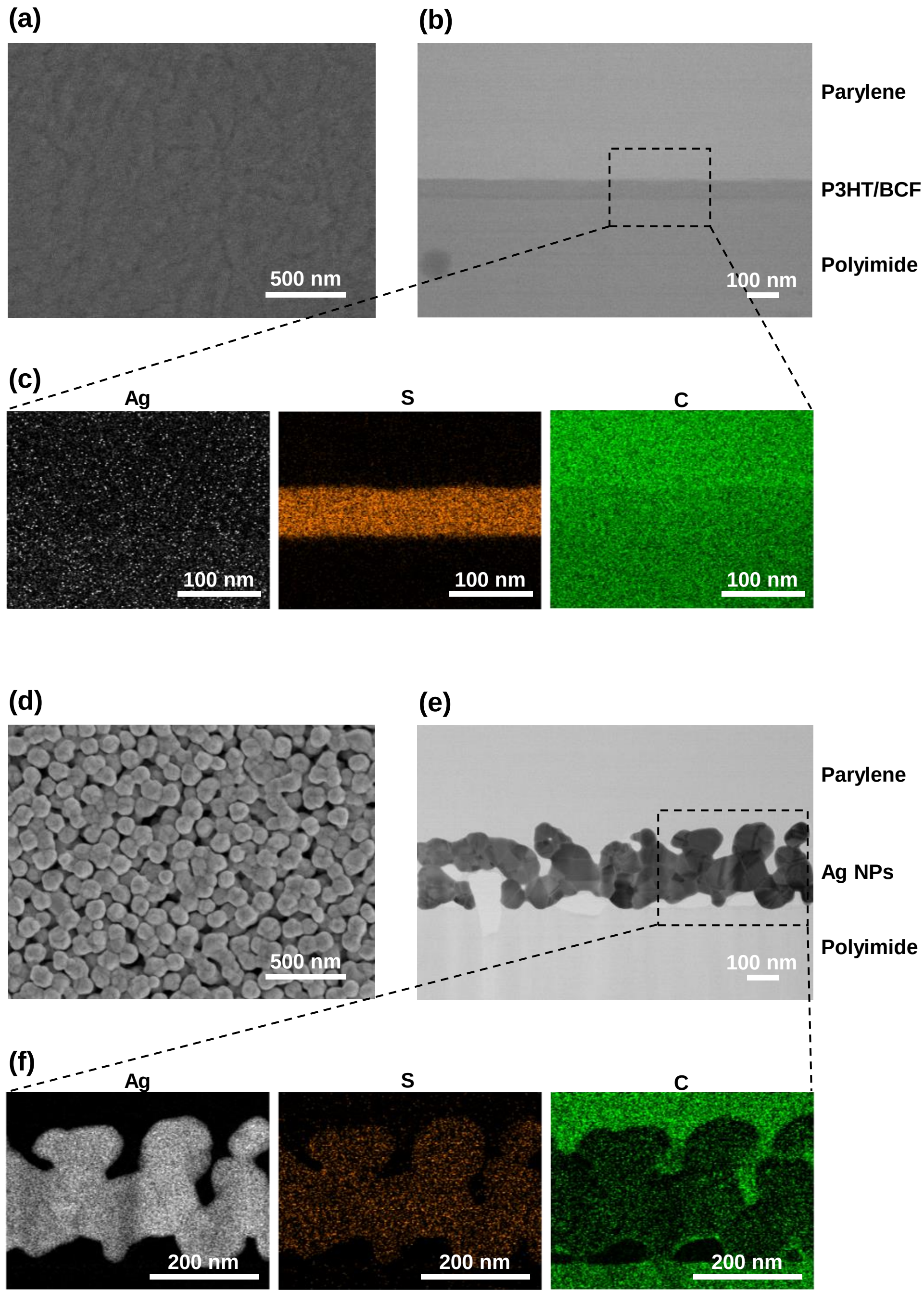

Fig. S1 Electron microscope images of nonhybrid films. (a–c) P3HT/BCF film without Ag NPs. (d–f) Ag NP film without P3HT and BCF. (a, d) SEM images of the films without parylene passivation observed from the surface. (b, e) Cross-sectional STEM images and (c, f) EDX elemental mapping images of the films. The elements are silver, sulfur, and carbon in order.

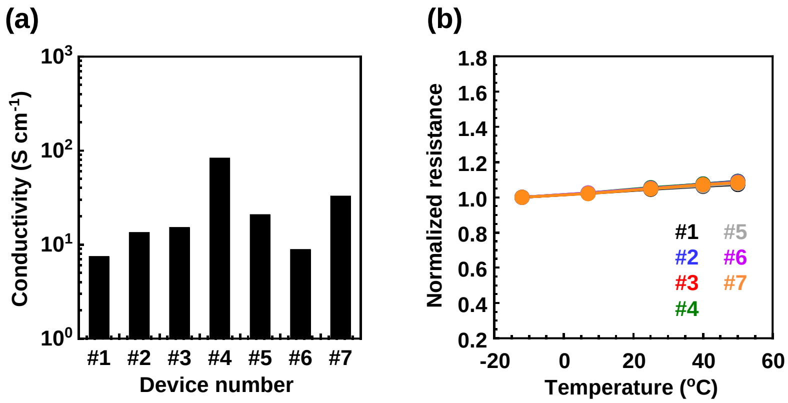

Fig. S2 Deviation of characteristics of seven near-zero-TCR strain sensors. (a) Conductivity of the sensors. (b) Resistance under different temperatures. The average value and standard deviation of TCR for the seven devices were 0.13% and 0.02% K^{-1}.

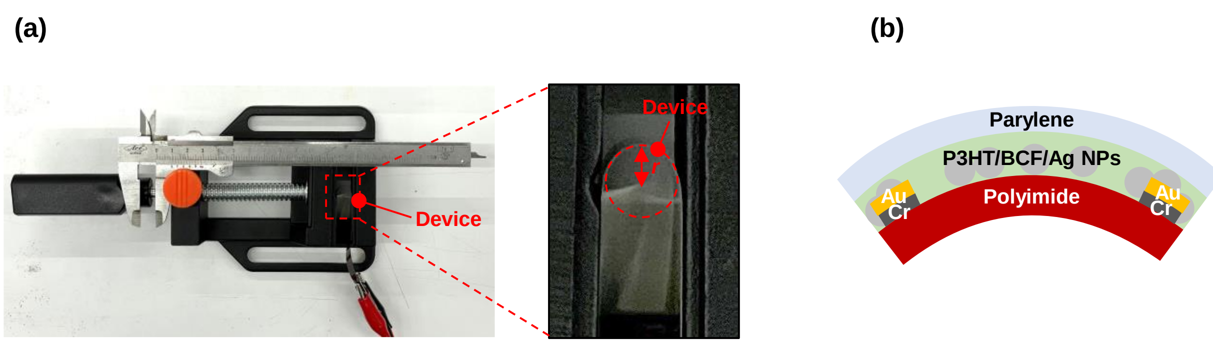

Fig. S3 Measurement method of strain sensors. (a) Photograph of the measurement system. (b) Schematic of the bent device that applies tensile strain to the sensor material.

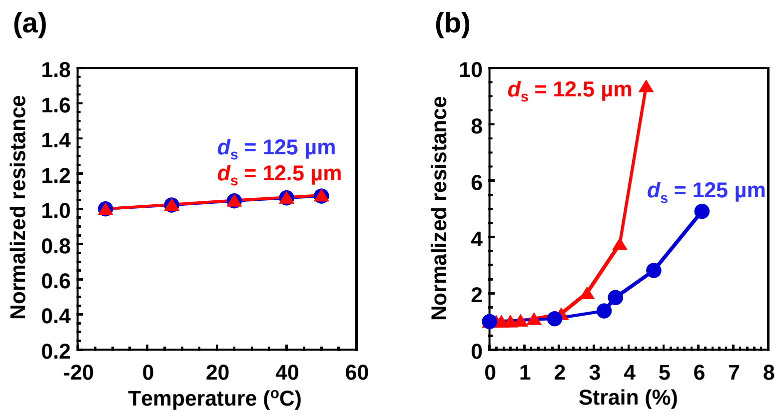

Fig. S4 Device characteristics of near-zero-TCR strain sensors for different substrate thickness. (a) Resistance under different temperatures. The TCR of the sensor with a substrate thickness of 12.5 µm was +0.11% K^{-1}. (b) Strain sensitivity of the sensors.

References

1 O. J. Gregory and X. Chen, in *2007 IEEE Sensors*, IEEE, 2007, pp. 624–627.

2 B. C. Marin, S. E. Root, A. D. Urbina, E. Aklile, R. Miller, A. V. Zaretski and D. J. Lipomi, *ACS Omega*, 2017, **2**, 626–630.

3 H. Gerdes, R. Bandorf, U. Heckmann, V. Schmidt, H.-U. Kricheldorf and G. Bräuer, *Plasma Process. Polym.*, 2009, **6**, S813–S816.

4 L. Yi, W. Jiao, C. Zhu, K. Wu, C. Zhang, L. Qian, S. Wang, Y. Jiang and S. Yuan, *Nano Res.*, 2016, **9**, 1346–1357.

5 M. Wen, X. Guan, H. Li and J. Ou, *Sensors Actuators A Phys.*, 2020, **301**, 111779.

6 R. Ramalingame, J. R. Bautista-Quijano, D. de F. Alves and O. Kanoun, *J. Compos. Sci.*, 2019, **3**, 96.

7 S. Harada, W. Honda, T. Arie, S. Akita and K. Takei, *ACS Nano*, 2014, **8**, 3921–3927.

8 S. Luo and T. Liu, *Adv. Mater.*, 2013, **25**, 5650–5657.

9 T. Park, H. K. Woo, B. K. Jung, B. Park, J. Bang, W. Kim, S. Jeon, J. Ahn, Y. Lee, Y. M. Lee, T. Kim and S. J. Oh, *ACS Nano*, 2021, **15**, 8120–8129.

10 Y. K. Choi, T. Park, D. H. D. Lee, J. Ahn, Y. H. Kim, S. Jeon, M. J. Han and S. J. Oh, *Nanoscale*, 2022, **14**, 8628–8639.

11 C. Wu, F. Lin, X. Pan, Y. Zeng, G. Chen, L. Xu, Y. He, G. He, Q. Chen, D. Sun and Z. Hai, *Chem. Eng. J.*, 2023, **457**, 141269.

12 Y. K. Choi, T. H. Kim, J. H. Song, B. K. Jung, W. Kim, J. H. Bae, H. J. Choi, J. Kwak, J. W. Shim and S. J. Oh, *Nanoscale*, 2023, **15**, 7980–7990.